NASA TECHNICAL TRANSLATION NASA TT F-14,796

STUDY OF THERMAL PHENOMENA IN A HARTMANN-SPRENGER TUBE

E. Brocher and C. Maresca

Translation of "Etude des phenomenes thermiques dans un tube de Hartmann-Sprenger", Int. J. Heat Mass Transfer, Vol. 16, [illegible] 1973 pp. 529-548

NATIONAL AERONAUTICS AND SPACE ADMINISTRATION
WASHINGTON, D. C. 20546 DECEMBER 1974

STANDARD TITLE PAGE

1. Report No.	2. Government Accession No.	3. Recipient's Catalog No.
NASA TT F-14,796		

4. Title and Subtitle	5. Report Date
STUDY OF THERMAL PHENOMENA IN A HARTMANN-SPRENGER TUBE	December 1974
	6. Performing Organization Code

7. Author(s)	8. Performing Organization Report No.
E. Brocher and C. Maresca	10. Work Unit No.

9. Performing Organization Name and Address	11. Contract or Grant No.
SCITRAN Box 5456 Santa Barbara, CA 93108	NASw-2483
	13. Type of Report and Period Covered
12. Sponsoring Agency Name and Address National Aeronautics and Space Administration Washington, D.C. 20546	Translation
	14. Sponsoring Agency Code

15. Supplementary Notes

Translation of "Etude des pheonomenes thermiques dans un tube de Hartmann-Sprenger", Int. J. Heat Mass Transfer, Vol. 16, 1973, pp. 529-548.

16. Abstract

Intense heating is generated in the Hartmann-Sprenger tube by shock waves and by friction of the oscillating gas against the tube walls. This heat is removed chiefly by mass exchange between the hot gas in the tube and the cold gas of the jet, but forced convection inside the tube is also important. Equilibrium temperature of the hot gas can be calculated by the theory developed here.

17. Key Words (Selected by Author(s))	18. Distribution Statement
	Unclassified - Unlimited

19. Security Classif. (of this report)	20. Security Classif. (of this page)	21. No. of Pages	22. Price
Unclassified	Unclassified	35	

PRECEDING PAGE BLANK NOT FILMED

STUDY OF THERMAL PHENOMENA IN A HARTMANN-SPRENGER TUBE

E. Brocher* and C. Maresca*

ABSTRACT. By directing a jet towards the entrance of a tube closed at the other end, strong flow oscillations may be obtained within the tube. The mechanical energy dissipated by friction on the tube walls, as well as by the irreversibility of the shock waves travelling up and down the tube, produces an important temperature increase of the oscillating gas and of the tube walls. The device is called "Hartmann-Sprenger tube".

The various removal mechanisms of the heat so produced are investigated. It is shown that the most important mechanism is a mass exchange between the gas of the jet (cold gas) and that oscillating within the tube (hot gas). This mass exchange occurs through the boundary layer thickness at the contact front separating the two gases.

The tube wall being alternately exposed to the hot and cold gases, heat transfer by forced convection occurs in the tube much as in a regenerative heat exchanger. A heat transfer balance is established and allows one to compute the equilibrium gas temperature. This temperature is markedly higher for monoatomic gases than for diatomic gases. The theoretical values of the equilibrium temperature are in good agreement with the experimental ones. The existence of a limiting Mach number of the hot gas flow is found.

* Institute for Fluid Mechanics, University of Provence, Marseille, France.

Notation

/529*

A — a/a_0;

D — hydraulic diameter of H-S tube;

C_f — coefficient of friction;

C_p — specific heat;

$I(K)$ — integral defined by Equation (A.4);

$I(M_2)$ — function defined by Equation (A.6);

K — parameter defined by Equation (10);

L — length of H-S tube;

L_p — depth of penetration of jet into tube;

M — Mach number;

Nu — Nusselt number;

P_2 — $p_2 u_2 S$;

P_{cf} — thermal power removed by forced convection inside tube;

P_{fr} — mechanical power dissipated by friction;

P_{irr} — mechanical power dissipated across shock waves;

P_m — thermal power removed by mass exchange;

Pr — Prandtl number;

Re — Reynolds number;

Re^* — $Dp_a/\mu_{tot_j}\sqrt{(RT_{tot_j})}$;

S — cross-sectional area;

T — static temperature;

T_F — wall temperature at bottom of tube;

T_r — recovery temperature of hot gas;

T_{tot} — stagnation temperature;

T_{tot_2} — mean stagnation temperature of hot gas

U — $(\gamma - 1)u/2a_0$;

a — speed of sound;

---

*Numbers in margin indicate pagination in original foreign text.

e — thickness of tube wall;

f — oscillation frequency;

h — heat transfer coefficient;

ℓ — distance between nozzle outlet and tube mouth;

m — $\rho_1 SL$, mass of gas contained in tube at start of compression phase; /530

m^* — mass transferred across contact front during compression phase;

p — stagnation pressure;

t — time;

u — gas velocity;

x — abscissa, measured from tube mouth;

y — distance of tube wall;

$\phi_m[\gamma, M_2, L/D, Re^*]$ — function defined by Equation (7);

$\phi_{cf}[\gamma, M_2, L/D, Re^*]$ — function defined by Equation (A.3);

$\phi_{irr}[\gamma, M_2]$ — function defined by Equation (14);

$\phi_{fr}[\gamma, M_2, L/D, Re^*]$ — function defined by Equation (A.8);

α — ratio of temperature of jet plenum to stagnation temperature of gas initially contained in tube;

γ — ratio of specific heats

$\delta(x)$ — boundary-layer thickness at abscissa x;

η — x/L_p;

θ — T_{tot_2}/T_{tot_j};

ν — kinematic viscosity;

ρ — density.

Subscripts

a — ambient conditions;

c.i. — incident shock wave;

c.r. — reflected shock wave;

d.i. — incident expansion wave;

d.r. — reflected expansion wave;

j — conditions at jet outlet;

1,2...7 — conditions in states 1, 2, ... 7, in Figure 2;

0 — reference conditions (conditions in jet plenum)
p — wall.

Introduction

By directing a jet of gas onto the mouth of a tube which is closed at its other end, it is possible to produce a strong oscillatory motion of the gas inside the tube. This phenomenon was discovered by Hartmann [1] in 1919, while he was making measurements of the pressure in a supersonic jet in the sub-accommodated regime with a Pitot tube. The oscillation of the gas produces loud sonic emission, with the dominant frequency near the fundamental acoustic frequency of the tube ($f = a/4L$). Hartmann and his collaborators went on to study the acoustic phenomena produced by this device more deeply. This is why it is customarily called the Hartmann whistle. It was only much later, in 1954, that Sprenger [2] showed that the oscillatory motion of the gas could produce considerable heating of the tube wall. In certain experiments by this author, the temperature of the wall reached 1000° C. Sprenger also showed that it is possible to obtain oscillation and heating of the tube wall with an exciting jet in the subsonic regime or in the accommodated supersonic regime. Discovery of the thermal effects created new interest in the Hartmann whistle, and many papers have been devoted to its study. In his paper, Sprenger [2] used the term "resonance tube"; since then this term has been taken up by most authors. However, as we have shown [3], this term is improper because even in the absence of friction or other dissipative processes, the maximum amplitude of the oscillations reaches a well-defined limiting value. During an international congress [4], we thus proposed to give the device the name "Hartmann-Sprenger tube" (H-S tube), and this suggestion has been favorably received.

Study of the thermal effects inside H-S tubes is interesting not only on a fundamental level, but also on a practical level. Sprenger [5] showed that serious accidents in the valving of pressurized gas can be blamed on these effects. He also showed [2] that it is possible to effect a "temperature separation": i.e., to /531

produce hot gas and cold gas from gas of intermediate temperature. Another application of the H-S tube consists of producing an oscillatory flow of 300° K plasma inside the tube, adequate for magnetohydrodynamic energy conversion [6].

The purpose of the present paper is to report the theoretical and experimental work which we have carried out on the thermal effects in H-S tubes at the Institute for Fluid Mechanics at Marseille during the last three years.

2. Operation of the H-S Tube

To begin the analysis of the thermal phenomena, it is essential to understand the nonviscous flow in a H-S tube. We have published a number of papers [3, 7, 8] on this subject, and we shall confine ourselves here to recalling the most important characteristics of the flow.

This can be divided into two phases (Figure 1). In the first phase, the jet penetrates into the tube and compresses the gas there. In the second phase, the tube empties, and the jet is pushed back some distance from the mouth.

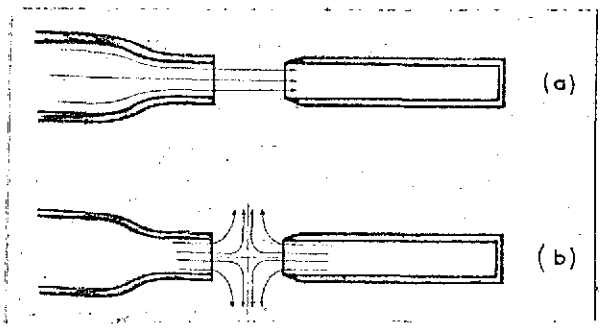

Figure 1. Phases of the flow in a H-S tube:
a — first phase: penetration of jet into tube; b — second phase: emptying of tube

It is advantageous to represent the instationary flow produced inside the tube by a time-distance diagram and a gas velocity-speed of sound diagram. In Figure 2, we have drawn one cycle of the oscillations in the time-distance diagram. The cycle is composed of an incident shock wave (o.c.i.), a reflected shock wave (o.c.r.), an incident expansion wave (o.d.i.), and a reflected expansion wave (o.d.r.). We note that it is the reflected shock wave which repels the jet outside the mouth, thus initiating the tube-emptying phase. We have also shown in the figure

the contact front (c.f.) between the gas of the jet and that contained in the tube. In a first analysis, it can be assumed that the pressure, temperature, and velocity are uniform in the flow regions numbered 1 to 7. We have demonstrated that if the condition necessary for starting and maintaining oscillation is satisfied [7], the amplitude of the oscillations tends to a limiting value for which the pressure behind the incident shock wave is just equal to the ambient pressure [3]. In Figure 3, we have used a gas velocity-speed of sound diagram to show the oscillation cycle when the limiting amplitude has been reached. The waves of compression and expansion (assumed isentropic) are governed by the Riemann invariants:

$$\left| \frac{2}{\gamma - 1} a \pm u \right| = \text{const.}$$

By introducing the dimensionless coordinates:

$$U = \frac{\gamma - 1}{2} \frac{u}{a_0}$$

$$A = \frac{a}{a_0}$$

these invariants are represented by straight lines of slope $\pm$ 1 in the A-U diagram. For the limiting cycle, the velocity in

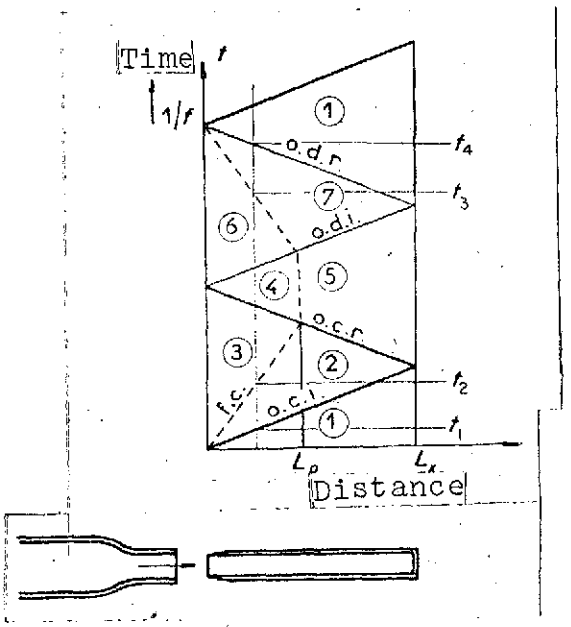

/532

Figure 2. Simplified time-distance diagram:

o.c.i. — incident compression wave; o.c.r. — reflected compression wave; o.d.i. — incident expansion wave; o.d.r. — reflected expansion wave; c.f. — contact front

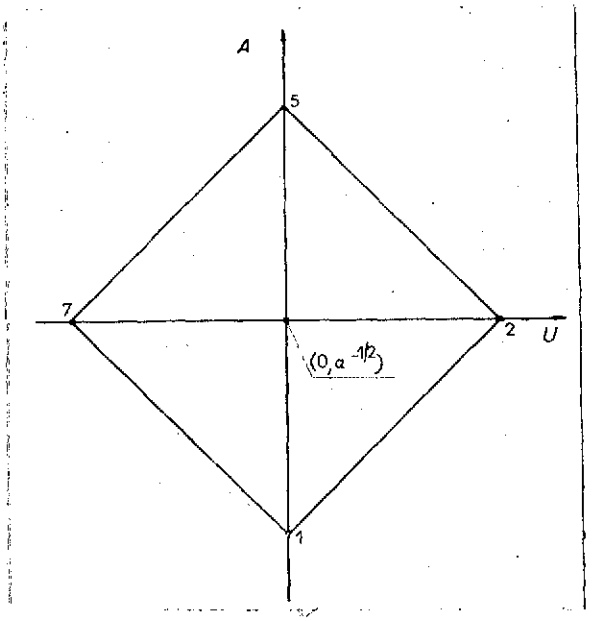

Figure 3. Limiting oscillation cycle:

1 - 2 — incident compression;
2 - 5 — reflected compression;
5 - 7 — incident expansion;
7 - 1 — reflected expansion

field 2 is equal to the velocity of the jet, which is to say that the jet penetrates freely into the tube. The jet is thus completely absorbed by the tube during the compression phase. The mechanism of oscillation is not significantly modified by irreversibilities (friction, shocks) which occur in real flow. Thus, the amplitude of the oscillations is always determined by the fact that when the limiting cycle is reached, the minimum pressure in the cycle adjusts itself in such a way that the pressure behind the incident shock is just equal to the ambient pressure. This condition allows the amplitude of the oscillations to be calculated immediately, when the exciting jet is in the accommodated supersonic regime and/or when the temperature of the gas in the tube is different from that of the jet [3].

3. Analysis of Prior Studies of Thermal Effects

Inspired by Sprenger's discovery [2], a number of authors [9 - 17] have sought to explain the thermal effects observed in H-S tubes.

The first question is that of knowing what the mechanisms are which produce the temperature rise. Most authors [9 - 16] suggest that the heating of the tube is due mainly to the dissipation of a part of the mechanical energy of the jet through the irreversibility of the shock waves present in the flow. Reynolds [17], on the other hand, attributes the dissipation to the turbulence of the flow inside the tube. In reality, we shall see later on that the two dissipative mechanisms, irreversibility of the shock waves and friction inside the tube, both play roles in raising the temperature. Their relative magnitudes depend mainly on the Mach number of the exciting jet, on the L/D ratio, and on the Reynolds number Re* defined below.

The second question is that of knowing what the mechanisms are which limit the temperature rise. Several authors [9, 13, 15, 16] suggest that the heat dissipated is transferred to the walls of the /533
tube by forced convection, and that this heat is then carried off in the atmosphere by radiation and free convection around the tube. They calculate the quantity of energy dissipated by the irreversibility of the shocks and compare it with the heat carried off. The

result of this comparison is relatively good [15], mediocre [9, 13], or plainly poor [16]. These divergences are due to the fact that the amount of energy dissipated in a shock wave depends, above all, on the pressure ratio p_5/p_1, and not on the pressure difference ($p_5 - p_1$). Now, measurement of pressure oscillations with a piezoelectric sensor does not generally, by itself, allow the determination of the absolute pressure, because of drift in the electronics. The authors mentioned were thus unable to calculate the irreversibilities due to the shocks with any certainty from their tests, as some of them pointed out themselves [9]. In addition, we shall see that in most cases, removal of heat by radiation and natural convection plays a minor role in the thermal balance of the tube.

Another mechanism which can limit the temperature rise is that proposed by Wilson and Resler [12]. The diagram of the flow in an H-S tube given in Figure 2 is very much simplified; in reality, passage from the expansion phase to the compression phase does not occur instantaneously, and a train of compression waves is formed at the mouth of the tube. This wave train moves a certain distance before it forms a shock. Wilson and Resler have shown that this formation distance increases with the temperature of the gas. Thus, insofar as the energy dissipation is due principally to the shock waves, the limiting temperature will be achieved when the wave train no longer has time to form a shock inside the tube. However, this mechanism is important only in determining the temperature reached at the bottom of the tube; we shall treat that question in another paper. We note that Wilson and Resler were unable to compare their theoretical result with experiment, since they did not have a sufficiently clear idea of the flow inside the tube.

Shapiro [14] attacked the problem of the formation of a shock in a gas containing a temperature gradient. In principle, this case is closer to reality than that studied by Wilson and Resler, for which the gradient was assumed to be zero. However, Shapiro's theory led to a much higher estimate of the temperature rise than that which is observed.

4. Preliminary Experiments

The various mechanisms for carrying off the heat produced by dissipation of the mechanical energy are exceedingly numerous, and it is judicious to proceed to experiments which allow one to judge which of them play major roles. Examination of the experimental results then allows establishment of a greatly simplified analysis of the thermal effects, which leads to theoretical values in good agreement with experiment.

4.1. Experimental systems

The experiments to be described were performed with two tubes, one rather large (tube No. 1), and the other small (tube No. 2).

For tube No. 1 (Figure 4), a compressor fills a series of compressed air cylinders B which are connected to the inlet pipe of nozzle T through plenum C. An electrically actuated valve E.V. is controlled by the quick-opening valve V_1. A pressure reduction valve Dt allows the generating pressure to be regulated between 1 and 15 bars. Valve V_2 provides fine regulation of the air flow in the piping system. Nozzle T, of square cross section, is easily interchangeable; its inlet section is a 60 x 60 mm square. The H-S tube is prismatic, with an internal length of 1200 mm; its cross section is 36 x 36 mm square. The L/D ratio is thus the same as that given by Sprenger [2] for obtaining the largest thermal effects. A system of tracks and ball /534

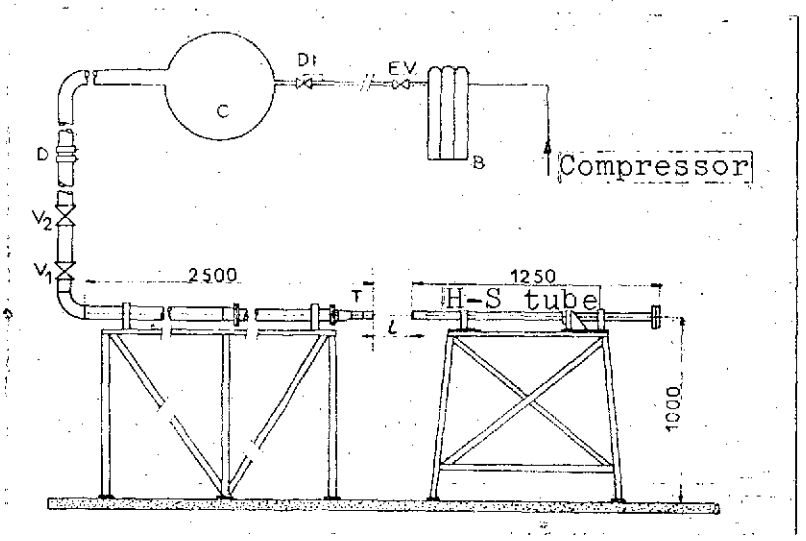

Figure 4. Experimental system (tube No. 1)

bearings allows the tube to slide on its support so that the distance l from the nozzle outlet to the tube mouth can be varied.

For tube No. 2 (Figure 5), the jet is supplied from one compressed gas cylinder B. The gas passes through a pressure reduction valve Dt which regulates the generating pressure, measured by manometer M in plenum C. Nozzle T and the H-S tube both have circular

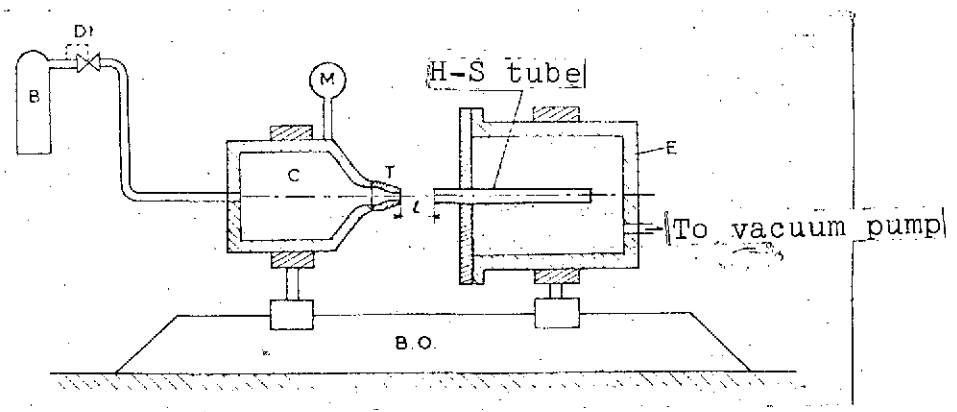

Figure 5. Experimental system (tube No. 2)

cross sections. The nozzle is interchangeable. The length of the tube is 100 mm. It is mounted in a cylindrical chamber E which can be evacuated in order to eliminate free convection around the tube. The plenum nozzle system and the tube chamber system are mounted coaxially on an optical bench BO, so that l can be varied easily.

4.2. Temperature measurement

We have made many temperature measurements using thermocouples placed in the wall of the tube, in order to determine the effects of various parameters and factors.

(a) Influence of geometric parameters. In general, it can be /535 said that the most important thermal effects are observed for geometric conditions similar to those required for obtaining the optimum amplitude of pressure oscillation [3, 7].

In all our experiments, the exciting jet was in the subsonic or adapted supersonic regime. In this case, the effect of the distance l separating the nozzle outlet from the tube mouth is much less important than in the case when the exciting jet is in the sub-accommodated supersonic regime [2]. For subsonic jets, thermal effects pass through a maximum for a value of l/D slightly larger than unity. For a Mach-2 supersonic jet, this maximum is observed at $l/D \approx 2$ when the gas is diatomic, and at $l/D \approx 3$ when the gas is monoatomic.

Temperature at the bottom of the tube is an increasing function of L/D, and reaches an effectively constant value for L/D > 30 (Figure 6).

The ratio of the jet cross section S_j to that of the tube mouth S must lie between 0.7 and 1 to obtain the largest thermal effects.

(b) Effect of roughness of the inner wall of the tube. For small tubes, this roughness plays a non-negligible role [18]. The observed temperature rise is slightly higher for a rough-walled tube than for a smooth-walled one.

(c) Effect of Mach number of exciting jet. In Figure 7, we have graphed the temperature distribution along an H-S tube for various Mach numbers M_j of the exciting jet. The temperature is an increasing function of M_j. It should be noted particularly that when M_j goes from 0.53 to 0.96, the temperature at x/L = 0.6 increases by only 30°, while at the bottom of the tube it increases by 160°. /536

(d) Effect of thermal insulation of the tube. Free convection and radiation around the outer wall of the tube are two mechanisms for removing the heat which can be reduced to a large extent. In a series of experiments carried out with the large H-S tube, the tube was insulated by a thick glass-wool sleeve.

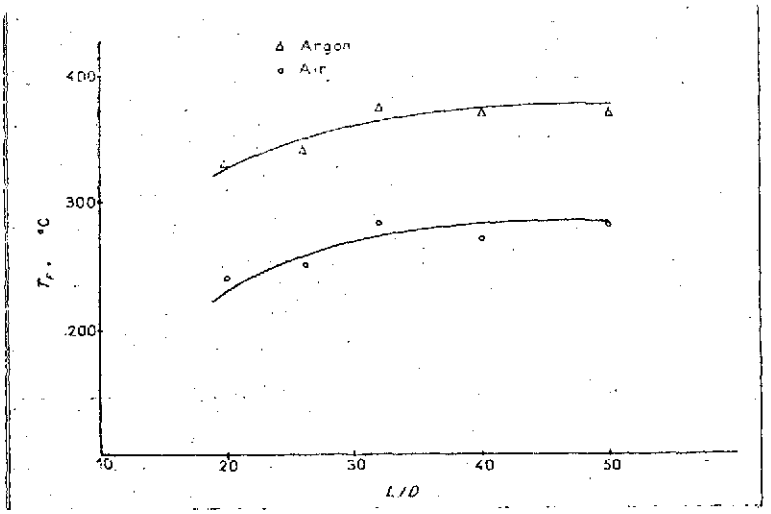

Figure 6. Effect of L/D ratio on temperature of wall at bottom of tube (tube No. 2: $S_j/S = 1$, $T_0 = 293°$ K, $M_j = 0.96$)

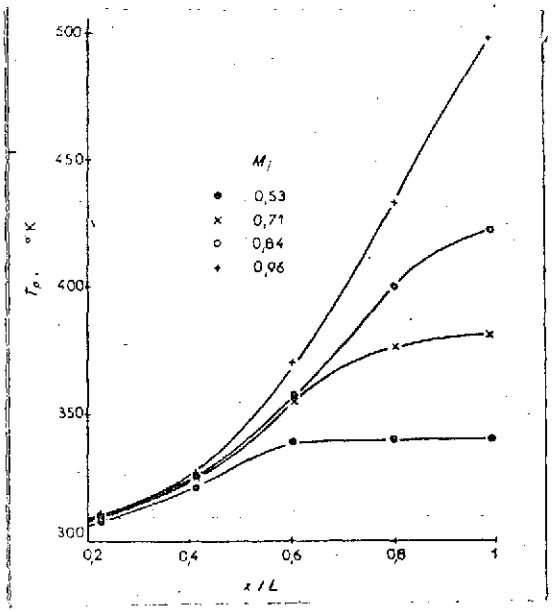

Figure 7. Effect of Mach number of exciting jet on distribution of wall temperatures of iron tube (tube No. 1: $S_j/S = 0.74$; $T_0 = 298°$ K; air)

In Figure 8 is graphed an example of the longitudinal temperature distribution for a supersonic exciting jet. It can be seen that exterior insulation is effective only at the bottom of the tube, where it produces an additional temperature rise of 120° C. In another series of experiments, carried out with tube No. 2, external thermal insulation also had a large effect only on temperatures at the bottom of the tube.

Because of the longitudinal temperature gradient, there is a flux of heat along the wall of the tube. This flux can be reduced by decreasing the thickness of this wall, and/or by

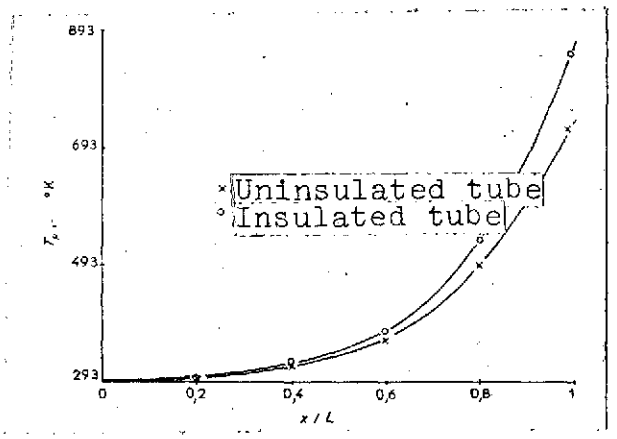

Figure 8. Effect of exterior thermal insulation of tube on distribution of wall temperatures of iron tube (tube No. 1: $S_j/S = 0.74$, $l/D = 2.4$; $T_0 = 298°$ K; air $M_j = 2$)

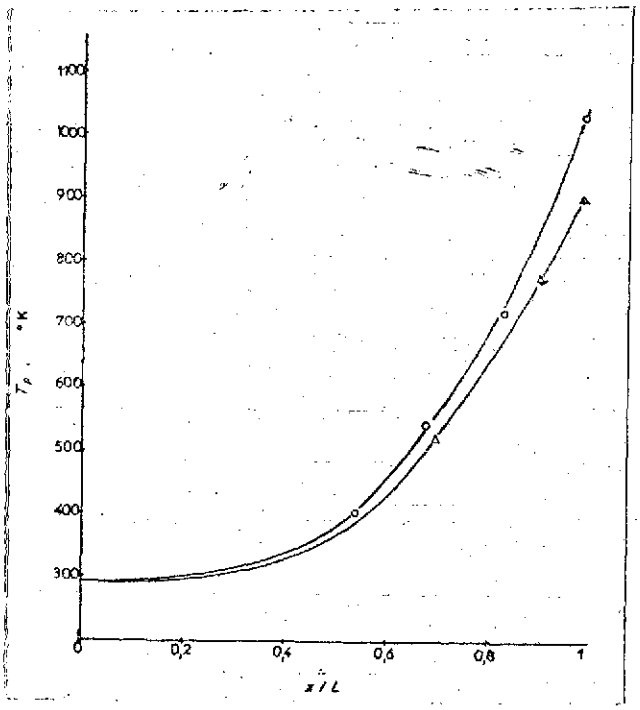

Figure 9. Effect of longitudinal heat conduction in tube walls (tube No. 2: $S_j/S = 1$; $T_0 = 293°$ K; helium; $M_j = 0.96$):
o — platinum tube (e = 1/10 mm;
Δ — iron tube (e = 5/10 mm)

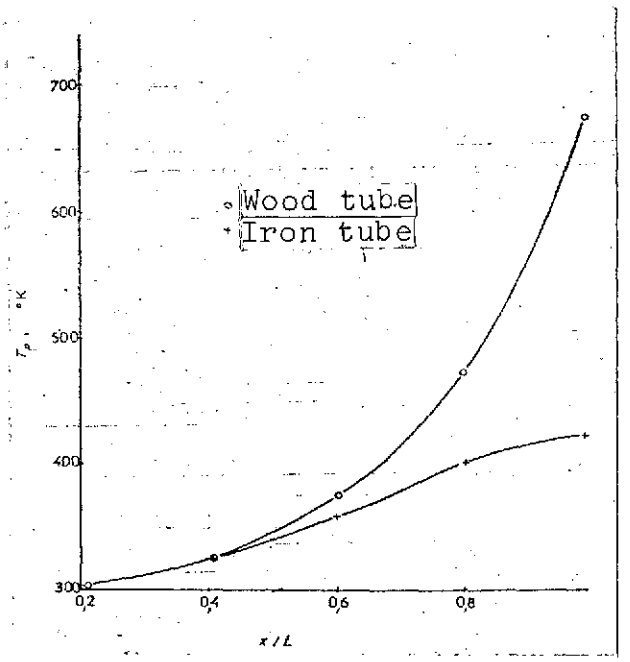

Figure 10. Effect of thermal insulation of the inner wall of tube (tube No. 1: $S_j/S = 0.74$, $T_0 = 293°$ K; air; $M_j = 0.84$)

choosing a material with low thermal conductivity. In Figure 9, results of two experiments are compared. In the first, the tube was made of iron, and its wall thickness was 5/10 mm. In the second, the tube was made of platinum, and its wall thickness was only 1/10 mm. It can be seen that the reduction in the longitudinal flux allows a considerable increase in the temperature at the bottom of the tube.

It can be supposed that transfer of gas to the inner wall of the tube can be reduced considerably if that wall is made of a good insulator. Experiments have thus been performed with various materials, particularly wood. Figure 10 compares temperatures measured in a wooden tube with those in an iron tube. It is seen that the increase in temperature due to the insulating nature of the wood is considerable at the bottom of the tube (250° K), but small out to $x/L \approx 0.6$. /537

(e) Effect of the nature of the gas. For certain applications [6, 19], it is necessary to consider use of other gases than air. Using hydrogen, Phillips and Pavli [19] measured a greater temperature rise than that obtained with nitrogen. We have proceeded to studies to determine the influence of the ratio of specific heats γ and of the molecular weight of the gas. Figure 11 shows the temperatures recorded for a tube excited by the following gases: helium, argon, air, and oxygen. The monoatomic gases are seen to produce a much greater temperature rise than do the diatomic gases. The effect of molecular weight of the gas used is small out to $x/L = 0.5$, but can be very large at the bottom of the tube.

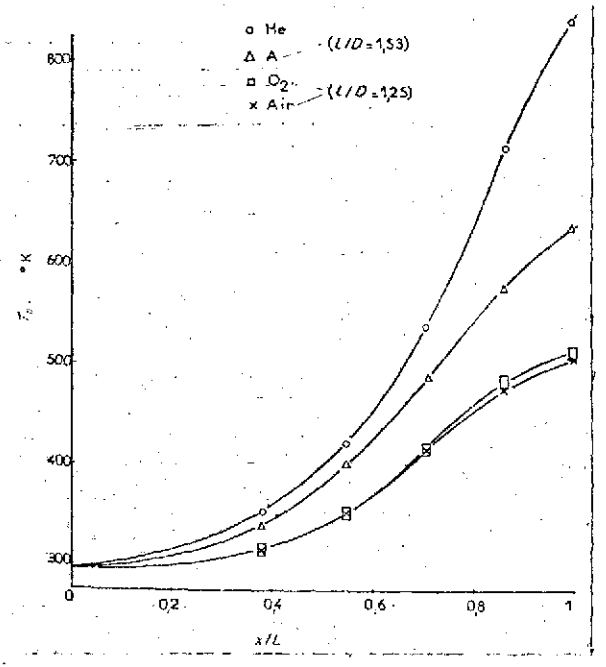

Figure 11. Effect of gas on thermal effects (tube No. 2: $S_j/S = 0.70$; $T_0 = 298°$ K; $M_j = 0.96$)

4.3. Hot-film records

Records have been made with hot-film gauges mounted on the tube wall. The film, about one micrometer thick, is formed of a deposit of platinum on a pyrex support. A record obtained for a supersonic Mach number is shown as an example in Figure 12. At the bottom of the tube, the behavior of the temperature variation is identical to that of the pressure variation [3]. /538

In the middle of the tube ($x/L = 0.5$), one can see the arrival of the incident shock, marked by temperature jump AB, a short plateau BC which corresponds to passage of the hot gas (state 2, Figure 2) over the gauge, cooling CD due to passage of the cold gas of the jet (state 3), then the arrival of the reflected shock, marked by

temperature jump De, followed by cooling FG which originates in the expansion which returns the temperature of the wall to its value in state 1.

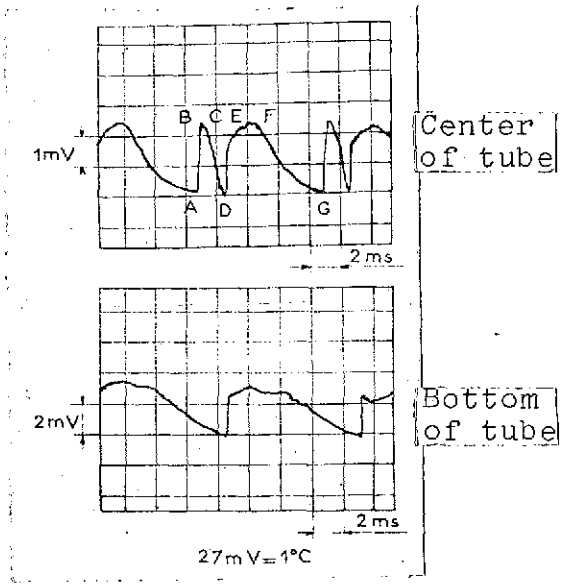

Figure 12. Hot-film records of tube wall (tube No. 1: $M_j = 2$)

4.4. Measurement of mass exchange between the gas of the exciting jet and the gas oscillating in the tube

As we shall explain in paragraph 5.1, there is a mass exchange across the contact front separating the gas of the exciting jet and the gas oscillating in the tube. This mass exchange can be revealed by exciting an initially air-filled H-S tube with a helium jet and following the time-dependence of the frequency of the oscillations in the tube [20]. The speed of sound in helium is considerably higher than in air. Thus, as the air in the tube is replaced by helium, the frequency of the oscillations increases.

To perform this experiment, the tube is suddenly set into operation by removing a shutter. The frequency of the oscillations is measured by displaying on a dual-trace oscilloscope the signal of a piezoelectric sensor mounted at the bottom of the tube. In the upper trace of Figure 13, one can see the beginning of the oscillations at the instant the shutter is opened, and the increase in their frequency with time. The lower trace allows examination of a selected portion of the upper trace, and allows more precise measurement of the variation of frequency with time. The analytical methods for this experiment are described in another paper [21].

5. Theory

5.1. Introduction

In light of the experimental results discussed above, it is possible to make the following statements:

a) Thermal insulation has little effect on the temperature rise of the wall in the region lying between $0 < x/L < 0.6$.

b) There is relatively large mass exchange between the gas of the jet and the gas oscillating in the tube.

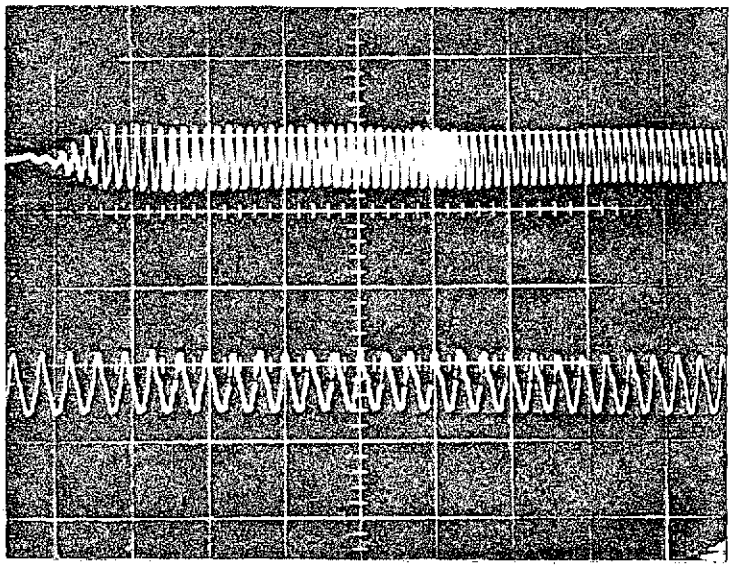

Figure 13. Change in frequency of oscillations, revealing mass exchange (tube No. 2, $M_j = 0.96$). Gas initially in tube: air; exciting gas: helium

This means both that the removal of heat by free convection and radiation around the tube plays a minor role in the region near the mouth, and also that the mass exchange can be an important mechanism of heat removal [22].

The mechanical energy dissipated by friction on the walls and by the irreversibility of the shock waves produces the heating of the gas oscillating in the tube. When thermal equilibrium is attained, the heat so produced in each cycle must be carried off, either by the walls of the tube or by the cold jet gas which penetrates the tube. Now, it is easy to demonstrate that, in general, the amount of heat carried off by free convection and radiation around the external wall of the tube is only a small percentage of

the mechanical energy dissipated [22]. Thus, to establish a thermal balance for the hot gas, it will suffice to consider the removal of heat by forced convection on the inner wall of the tube and by mass exchange between the hot gas and the cold gas.

The temperature of the hot gas is certainly not uniform. In fact, while the amplitude of the pressure oscillations and, consequently, the intensity of the shock waves are nearly constant along the tube, the amplitude of the oscillatory movement is a decreasing function of the abscissa, and becomes zero at the bottom of the tube. From this it results that the irreversibility of the shock waves produces uniform heating of the gas (if the formation length of the shock wave is small with respect to the length of the tube), but that the magnitudes of the friction and of the forced convection vary with /539 the abscissa. An exact calculation of the temperature distribution in the hot gas runs into considerable difficulty. The overall thermal balance of the hot gas, which we shall establish in this section, does not allow the average temperature of the gas to be determined with good accuracy.

5.2. Mass exchange

During penetration of the jet into the tube, a certain mass m* of hot gas passes through the contact front within the thickness of the boundary layer. This phenomenon is analogous to that observed in shock tubes [23]. During the phase in which the tube is evacuated, it is an equal mass of cold gas which passes through the contact surface and mixes with the hot gas. These two processes are easily understood when they are visualized in a coordinate system fixed to the contact front. In this system, the boundary layer has the behavior shown by Figure 14. While the theoretical determination of m* is easy under certain hypotheses, its experimental verification is more difficult [21].

For the experimental conditions described above, the Reynolds numbers are high, and the flow is turbulent. The theoretical study of the boundary layer in a H-S tube is complex, because the flow is

unstationary. It is reasonable, however, to think that at each cycle during the compression phase, a boundary layer is established, starting from the mouth. If we assume that this boundary layer develops as it does on a plane plate in steady turbulent flow, the velocity profile is then given by:

$$\frac{u}{u_2} = \left(\frac{y}{\delta}\right)^{\frac{1}{7}} \tag{1}$$

where y represents the distance of the tube wall, and δ — the thickness of the boundary layer at abscissa x, i.e.,

$$\delta(x) = 0{,}37x\left(\frac{u_2 x}{\nu_2}\right)^{-\frac{1}{5}} \tag{2}$$

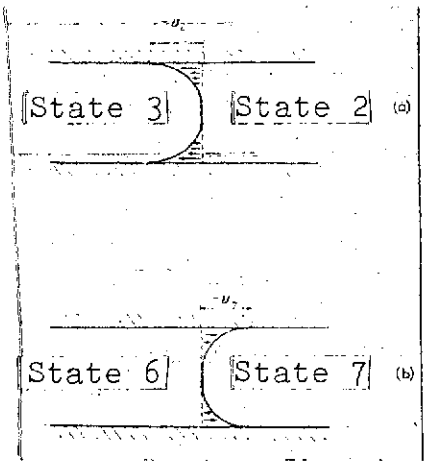

Figure 14. Boundary-layer profiles in a system of coordinates fixed to the contact front:
(a) — during compression phase; (b) — during emptying phase

With this simplified model, the mass percentage of hot gas which passes across the contact front within the thickness of the boundary layer is given by [21]:

$$\frac{m^*}{m} = 0{,}103\left(\frac{\rho_2}{\rho_1}\right)\left(\frac{L_p}{L}\right)^5\left(\frac{L}{D}\right)^{\frac{4}{5}}(Re_2)^{-\frac{1}{5}} \times\left[1 - 0{,}137\left(\frac{L_p}{L}\right)^{\frac{4}{5}}\left(\frac{L}{D}\right)^{\frac{4}{5}}(Re_2)^{-\frac{1}{5}}\right] \tag{3}$$

where $Re_2 = u_2 D/\nu_2 \cong (\sqrt{\gamma})\, M_2 Re^*$. The ratio m*/m is a function of the Mach number M_2 of the flow in state 2 (Figure 2). Now, the ratio ρ_2/ρ_1 is given by the Hugoniot relations. And also, the penetration depth L_p is given by:

$$\frac{L_p}{L} = \frac{\frac{a_2}{u_{ci}} + \frac{a_2}{u_{cr}}}{\frac{1}{M_2} + \frac{a_2}{u_{cr}}} \tag{4}$$

The Hugoniot equations also allow the ratios a_2/u_{ci} and a_2/u_{cr} to be

expressed as functions of M_2, and thus allow L_p/L to be calculated as a function of M_2. The result of these calculations is given in Figure 15. They have been performed for $\gamma = 7/5$ and $6/3$, but the difference between the values obtained is so small that a single curve has been drawn. It can be seen that the depth of penetration increases rapidly with M_2, and this allows a better understanding of the importance of heat removal by mass exchange and by forced convection inside the tube. /540

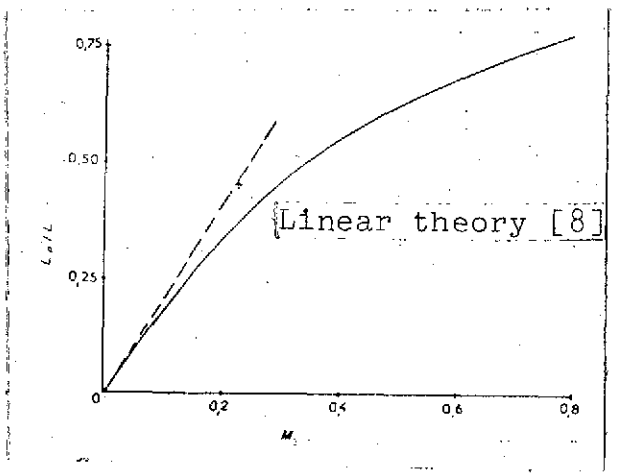

Figure 15. Depth of jet penetration into tube

Note also that the theoretical values of m*/m given by Equation (3) are in good agreement with the experimental values [21].

5.3. Energy transferred from hot to cold gas by mass exchange

The mass m* of hot gas passing across the contact front carries away with it an enthalpy equal to $m^*C_p T_{tot_2}$, where T_{tot_2} is the average stagnation temperature of the hot gas. During expansion, an equal mass of cold gas is substituted for that previously given up, and carried with it an enthalpy equal to $m^*C_p T_{tot_1}$. Thus, the amount of heat Q_m lost by the hot gas during one cycle is:

$$Q_m = m^*C_p(T_{tot_2} - T_{tot_1}). \qquad (5)$$

Noting that the period of the oscillations is effectively equal to $4L/a_2$, the energy P_m transferred per unit time is $P_m \cong Q_m a_2/4L$. On relating P_m to the maximum mechanical power P_2 which can be transferred by compression from the jet gas to the gas contained in the

tube, we obtain:

$$\frac{P_m}{P_2} = \phi_m[\gamma, M_2, L/D, Re^*]\left(\frac{\theta - 1}{\theta}\right) \tag{6}$$

where $\theta = T_{tot_2}/T_{tot_1}$, and

$$\phi_m = \frac{1}{4}\left(\frac{\gamma}{\gamma - 1}\right)\left(\frac{m^*}{m}\right)\left(\frac{\rho_1}{\rho_2}\right) \times \left(\frac{1 + \left(\frac{\gamma - 1}{2}\right)M_2^2}{M_2}\right), \tag{7}$$

(m*/m) being given by Equation (3).

5.4.. Heat transfer by forced convection inside the tube

For $M_2 > 0.4$, when the limiting cycle is reached, the jet gas penetrates deep into the tube (Figure 15). Up to the penetration depth L_p, the tube wall is swept alternately by the hot gas of the cavity and the cold gas of the jet. At a given abscissa, the wall receives a certain amount of heat from the hot gas and returns it to the cold gas when thermal equilibrium is reached at the wall; heat conduction along the wall plays a minor role. It should be noted that almost all this heat does not pass through the wall from one side to the other, and that external thermal insulation of the tube thus does not reduce the magnitude of this mechanism of heat removal at all. The wall acts as a heat sink, just as in regenerative heat exchangers.

For precise determination of the heat transfer from the hot gas to the wall by forced convection, it would be necessary to know the exact development of the boundary layer in this gas. As we have already mentioned above, calculation of this boundary layer would be very complex, and it is preferable to try to apply known relations, using certain hypotheses. Unlike what occurs in a shock tube where the gas is at rest before the passage of the shock wave, and where /541
the boundary layer is formed at the base of the shock, these already exist before the shock passes, because of the oscillatory character of the flow of the hot gas. We thus make the hypothesis that the

heat transfer is practically equal to that of a completely developed permanent flow. This hypothesis leads to theoretical results in good agreement with experiment [24].

Let $T_p(x)$ be the temperature of the wall at abscissa x, T_r — the recovery temperature of the hot gas, and h_2 — the heat transfer coefficient to the wall. During times $(t_2 - t_1)$ and $(t_4 - t_3)$ (cf. Figure 2), the hot gas gives up to the surface π D dx of the tube the amount of heat dQ_{cf}:

$$dQ_{cf} = [h_2(t_2 - t_1) + h_2(t_4 - t_3)] \times [T_r - T_p(x)]\pi D\, dx.$$

We assume $h_2 \approx h_2$ and $(t_2 - t_1) \approx (t_4 - t_3)$. During one period, the amount of heat given up by the hot gas to the wall is thus:

$$Q_{cf} \cong 2\pi D h_2 \int_0^{L_p} [T_r - T_p(x)](t_2 - t_1)\, dx. \tag{8}$$

Noting that $(t_2 - t_1) = x(1/u_2 - 1/u_{ci})$, and that the period of the oscillations is practically equal to $4L/a_2$, the thermal power carried off by forced convection inside the tube (with respect to P_2) is:

$$\frac{P_{cf}}{P_2} = \frac{2h_2}{p_2 u_2}\left(\frac{L}{D}\right)\left(\frac{L_p}{L}\right)^2\left(\frac{1}{M_2} - \frac{a_2}{u_{ci}}\right) \times \int_0^1 [T_r - T_p(x)]\,\eta\, d\eta \tag{9}$$

where $\eta = x/L_p$. We have shown [24] that the longitudinal variation of the wall temperature is given by:

$$\frac{T_p(x) - T_{tot_1}}{T_p(L_p) - T_{tot_1}} = \frac{K\eta^{\frac{1}{2}}}{1 - \eta + K\eta^{\frac{1}{2}}}$$

where

$$K = 0{,}795\,(Pr)^{0,3}(L_p/L)^{\frac{1}{2}}(L/D)^{0,2} \times (1/u_2 - 1/u_{ci})/(1/u_{ci} + 1/u_{cr}). \tag{10}$$

It seems reasonable to make the hypothesis that the temperature of the wall at L_p is nearly equal to the temperature of the hot gas, since beyond this abscissa the wall is swept only by this gas. With this hypothesis, and setting $T_r \cong \theta T_{tot_j}$, we have:

$$T_r - T_p(x) = T_{tot_j}(\theta - 1)\left[\frac{1-\eta}{1-\eta+K\eta^{\frac{4}{5}}}\right]. \qquad (11)$$

The coefficient h_2 is given by the well-known empirical formula [25]:

$$h_2 = 0{,}023\,\frac{k_2 (Re_2)^{0.8}\,(Pr)^{0.4}}{D}. \qquad (12)$$

It is demonstrated in the Appendix that with the aid of Relations (11) and (12), Equation (9) can be put into the form:

$$\frac{P_{cf}}{P_2} = \phi_{cf}[\gamma, M_2, L/D, Re^*]\left(\frac{\theta - 1}{\theta}\right). \qquad (13)$$

5.5. Mechanical energy dissipated across the shock waves

During one cycle, the gas oscillating in the tube is run through by a shock wave and its reflection, then by a bundle of expansion waves and its reflection. Although the expansion waves are isentropic (effects of wall friction are considered separately below), it is not the same for the shock waves. To calculate the mechanical energy thus dissipated, it is advantageous to represent the cycle in a temperature-entropy diagram (Figure 16). The incident shock wave brings the gas from state 1 to state 2, and its reflection from state 2 to state 5. If no heat is removed, the isentropic expansion will bring the gas to state 1'. In order to close the cycle, it is necessary to remove an amount of heat to make the gas go from state 5 to state 5', for example.

Let Q_{irr} be the mechanical energy dissipated by the irreversibility of the shock waves at each cycle: /542

$$Q_{irr} = mC_p \Delta T_5$$

where $\Delta T_5 = (T_5 - T_{5'})$. Noting that the frequency of the oscillations is practically equal to $a_2/4L$, the mechanical power dissipated by the irreversibility of the shock waves, with respect to P_2, becomes:

$$\frac{P_{irr}}{P_2} = \frac{\gamma}{4(\gamma - 1)} \frac{(p_1/p_2)(\Delta T_5/T_1)}{M_2} = \phi_{irr}[\gamma, M_2] \qquad (14)$$

because (p_1/p_2) and $(\Delta T_5/T_1)$ are functions of M_2.

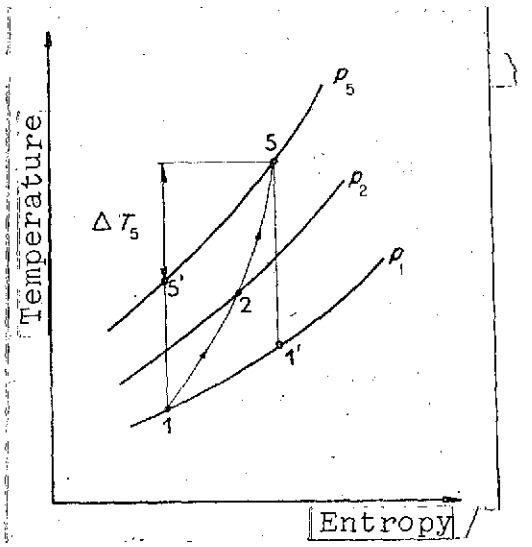

Figure 16. Incident and reflected shock waves in the temperature-entropy diagram

5.6. Mechanical energy dissipated by friction

Let us consider the simplified wave diagram (Figure 2), and place ourselves at abscissa x of the tube. Let C_{f2} be the coefficient of friction, and u_2 — the mean velocity of the gas in the section considered. During time $(t_2 - t_1)$, the total energy dQ_{fr} dissipated by friction on an element of wall of length dx is:

$$\frac{C_{f_2}}{2} \rho_2 u_2^3 \frac{S}{D} (t_2 - t_1)\, dx.$$

If we assume that the energy dissipated during time $(t_4 - t_3)$, during the expansion, is nearly equal to that dissipated during time $(t_2 - t_1)$, the total energy dQ_{fr} dissipated by friction on an element of wall of length dx is then:

$$dQ_{fr} = C_{f_2} \rho_2 u_2^3 \frac{S}{D} (t_2 - t_1)\, dx.$$

Integrating over the length of the tube and dividing by the period $4L/a_2$, the total power dissipated by friction, with respect to P_2, becomes:

$$\frac{P_{fr}}{P_2} = \frac{\gamma}{4LD} C_{f_2} M_2^2 a_2 \int_0^L (t_2 - t_1)\,dx. \tag{15}$$

Time $(t_2 - t_1)$ is a function of x, and of the velocities u_{ci}, u_{cr}, and u_2:

for
$$0 \leqslant x \leqslant L_p$$
$$(t_2 - t_1) = x\left(\frac{1}{u_2} - \frac{1}{u_{ci}}\right) \tag{16a}$$

for
$$L_p \leqslant x \leqslant L$$
$$(t_2 - t_1) = (L - x)\left(\frac{1}{u_{ci}} + \frac{1}{u_{cr}}\right) \tag{16b}$$

For the coefficient of friction C_{f2}, we use the same hypothesis as that used previously for the heat transfer coefficient, namely, that the coefficient is practically equal to that for a completely developed stationary flow. Thus, we write:

$$C_{f_2} = 0.316 Re_2^{-0.25} \tag{17}$$

Introducing Relations (16a), (16b), and (17) into Equation (15), the power dissipated by friction can be put into the form (see Appendix):

$$\frac{P_{fr}}{P_2} = \phi_{fr}[\gamma, M_2, L/D, Re^*]. \tag{18}$$

5.7. Thermal balance

As we have shown above, the mechanical energy dissipated by friction on the walls of the tube and by the irreversibility of the shock waves produces heating of the gas in the tube. This heating /543 is limited mainly by heat removal through mass exchange and through

forced convection at the inner walls of the tube. Thermal equilibrium is thus attained when:

$$P_m + P_{c.f.} = P_{irr} + P_{fr} \tag{19}$$

Using Equations (6), (13), (14), and (18), this thermal balance takes the form:

$$(\phi_m + \phi_{c.f.})\left(\frac{\theta - 1}{\theta}\right) = \phi_{irr} + \phi_{fr}$$

The average temperature of the hot gas when thermal equilibrium is reached is thus given by:

$$\theta = \left[1 - \frac{\phi_{irr} + \phi_{fr}}{\phi_m + \phi_{c.f.}}\right]^{-1} \tag{20}$$

The functions ϕ_{irr}, ϕ_{fr}, ϕ_m, and $\phi_{c.f.}$ are shown in Figures 17 and 18 for air and helium, respectively. It can be seen that ϕ_{irr} and ϕ_{fr} are increasing functions, while ϕ_m and $\phi_{c.f.}$ are decreasing functions of M_2. It can easily be verified that when M_2 approaches

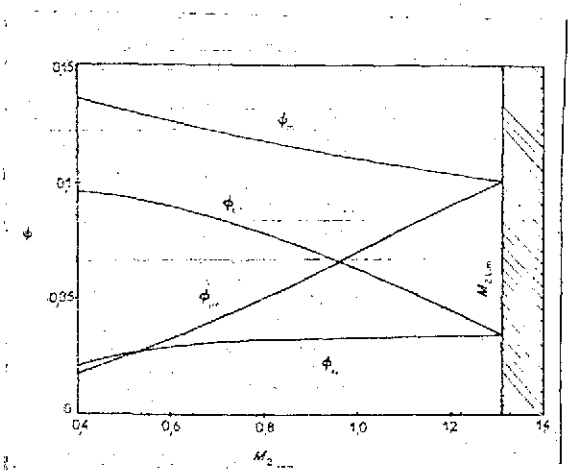

Figure 17. $\phi(M_2)$ functions for air (L/D = 33)

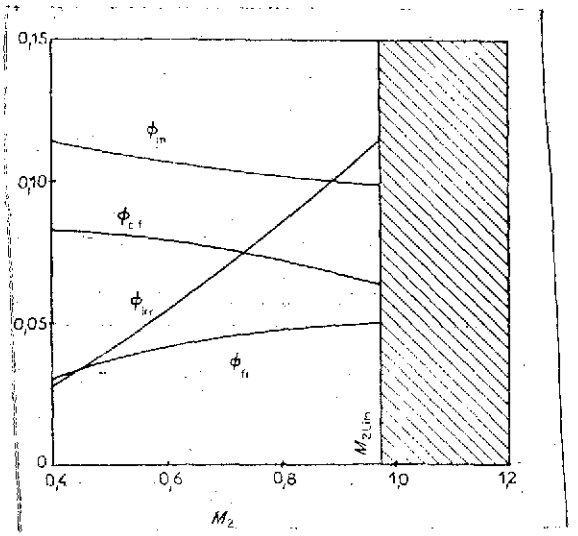

Figure 18. $\phi(M_2)$ functions for for helium (L/D = 33)

the limiting value $M_{2\ lim}$, the quotient $(\phi_{irr} + \phi_{fr})/(\phi_m + \phi_{c.f})$ approaches unity. Thus, according to Equation (20), θ could become infinite. But there is another relation which must be taken into consideration.

When the limiting cycle is reached [3], the velocity u_2 is determined uniquely by the velocity of the jet, and thus is not affected by the rise in the temperature of the gas oscillating in the tube. In contrast, a_2 is an increasing function of T_{tot_2}, and it follows that M_2 is a decreasing function of θ. For given S_j/S and M_j, the relation between θ and M_2 is [20]:

$$\theta = \left(\frac{S_j}{S}\right)^2 \left(\frac{M_j}{M_2}\right)^2 \times \frac{\left(1 + \frac{\gamma - 1}{2} M_2^2\right)\left(1 + \frac{\gamma - 1}{2} M_j^2\right)}{\left(1 + \frac{S_j}{S}\frac{\gamma - 1}{\gamma} M_j^2\right)^2} \tag{21}$$

The $\theta(M_2)$ curve representing Equation (20), and the $\theta(M_2, M_j)$ curve representing Equation (21) are drawn in Figure 19. The point of intersection of the $\theta(M_2)$ curve with the $\theta(M_2, M_j)$ curve corresponds to the operating point at thermal equilibrium for a given M_j. It can be seen that the value of M_2 at equilibrium is an increasing function of M_j, but always remains less than $M_{2\ lim}$. θ is thus an increasing function of M_j, but tends toward infinity only when M_j tends toward infinity.

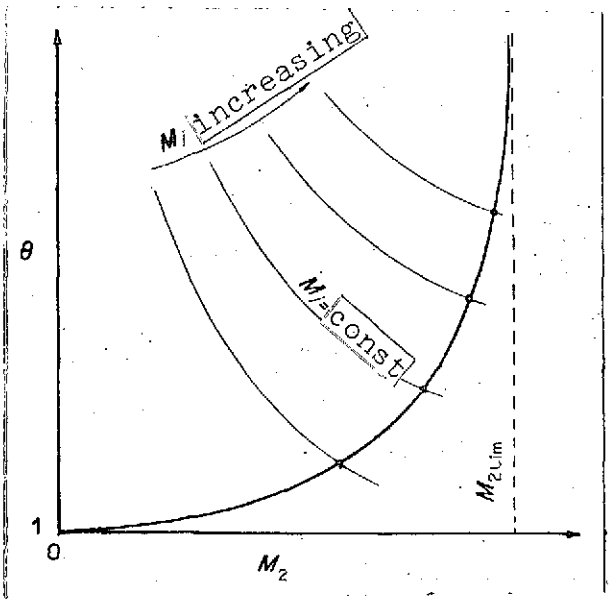

Figure 19. Graphic solution of thermal balance

/544

6. Comparison of Theoretical and Experimental Results

The purpose of the preliminary experiments (section 4) was the determination of those parameters and mechanisms which play important roles in the thermal effects observed in H-S tubes. They allowed us to make simplifying hypotheses and to establish a thermal balance for the hot gas.

The experiments described below were intended to determine whether the temperature measured at thermal equilibrium is in good agreement with the theoretical value given by the balance. We used tube 2 for these tests in order to limit consumption of helium and argon.

The thermal balance was established for the case where the tube /545
is essentially adiabatic. Now, for tubes of small dimensions, free convection and radiation play non-negligible roles when the wall temperature rises above a certain level. Therefore, we have always evacuated the chamber around the tube, but it would also be desirable to be able to place a reflecting screen around the tube to reduce radiation losses. A platinum tube was used, with a wall thickness of only 1/10 mm, to reduce losses by longitudinal conduction.

The theoretical analysis shows that the equilibrium temperature θ depends on the geometry (L/D), on the nature of the gas (γ, Re*), and the Mach number M_j. For each experiment, we can calculate θ by means of Equations (20) and (21). An M_2 and, consequently, a penetration depth L_p correspond to this value of θ (Figure 15).

Temperature measurements by thermocouples allow one to trace the temperature distribution as a function of the abscissa. Now, we have seen (paragraph 5.4) that the wall temperature at L_p must be practically equal to the temperature of the hot gas. We are thus able to compare the wall temperature measured at depth L_p calculated above,

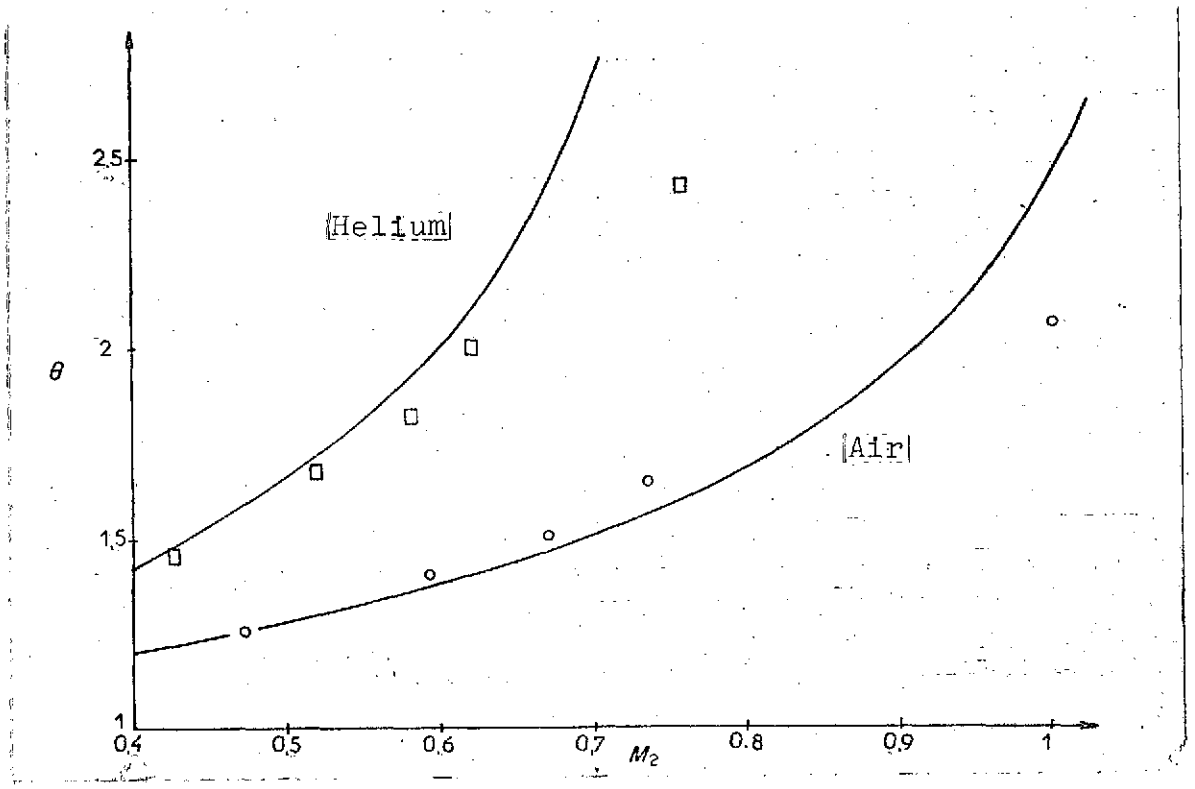

Figure 20. Comparison of theoretical and experimental values of θ (tube No. 2)

and temperature θ given by the thermal balance. This comparison is shown in Figure 20 for air and helium.

Theory and experiment show that the thermal effects are much larger in monoatomic gases than in diatomic gases. Theoretical and experimental values of θ agree well for $\theta < 2$. For $\theta > 2$, the effect of heat loss by radiation is non-negligible, and the experimental values of θ are smaller than the theoretical values.

7. Conclusions

In this paper, we have analyzed the various mechanisms for the dissipation of mechanical energy and the removal of heat which takes place in a Hartmann-Sprenger tube. It has been demonstrated that friction on the walls and the irreversibility of the shock waves are of comparable importance in the dissipation of mechanical energy into heat. Free convection and radiation around the outer wall of

the tube, as well as thermal conduction along the wall, are non-negligible only for the temperatures observed at the bottom of the tube, expecially for tubes of small dimensions.

Forced convection inside the tube is important, but it is principally the exchange of mass between the cold gas of the jet and the hot gas oscillating in the tube which limits the temperature rise observed in H-S tubes.

The equilibrium temperature of the hot gas can be calculated by means of the thermal balance, and the theoretical results obtained in this way agree well with the experimental values. It has been demonstrated that the thermal effects are much greater in monoatomic gases than in diatomic gases. The existence of a limiting Mach number for the flow of the hot gas has been shown.

The results obtained allow consideration of interesting applications of the H-S tube in high temperature chemistry and in magneto-hydrodynamic energy conversion.

Acknowledgements

The authors wish to thank M. M. Albertini, who made many of the measurements reported in this paper.

References

1. Hartmann, J. A new method of Frembringel and Lydsvinginger. Dan. Mat. Fys. Medd. Vol. 1, 1919.

2. Sprenger, H. On Thermal Effects in Resonance Tubes. Mitteilungen aus dem Institut fuer Aerodynamik, E. T. H. Zurich, No. 21, 1954, pp. 18-35.

3. Brocher, E., C. Maresca and M. H. Bournay. Fluid Dynamics of the Resonance Tube. J. Fluid Mech., Vol. 43, No. 2, 1970, pp. 369-384.

4. Rott, N. and H. Thomann. Finite Amplitude and Diffusive Effects in Acoustics: A Report on EUROMECH 23. J. Fluid Mech., Vol. 49, No. 2, 1971, pp. 391-397. /546

5. Sprenger, H. New Knowledge About the Thermal Effects of the Expansion of Gases. Journal de la Soudure, No. 10, 1956, pp. 3-15.

6. Brocher, E. and C. Maresca. Pulsed Flow of a Plasma in a Resonance Tube and Application to a Shock-Wave M.H.D. Generator. Proceedings of the Fifth International Conference on Magnetohydrodynamic Electrical Power Generation, Munich, 1971, pp. 551-561.

7. Brocher, E. and C. Maresca. Operating Condition of a Resonance Tube Sustained by a Subsonic Jet. C. R. Acad. Sci., Vol. 268A, 1969, pp. 749-752.

8. Brocher, E. and C. Maersca. Studies of Resonance Tubes Excited by a Subsonic Jet. J. Mechanique, Vol. 8, 1969, pp. 21-39.

9. Howick, P. and R. Hughes. Pressure and Temperature Effects in Resonance Tubes. S.B. Thesis, Massachusetts Institute of Technology, 1958.

10. Sibulkin, M. and T. Vrebalovich. Some Experiments with a Resonance Tube in a Supersonic Wind Tunnel. J. Aero. Sci., Vol. 25, 1958, pp. 465-466.

11. Hall, I. M. and C. J. Berry. On the Heating Effect in a Resonance Tube. J. Aerospace Sci., Vol. 26, No. 4, 1959, p. 253.

12. Wilson, J. and E. L. Resler. A Mechanism of Resonance Tubes. J. Aerospace Sci., Vol. 26, No. 7, 1959, pp. 461-462.

13. Shapiro, A. H. Shock Waves and Dissipation in a Resonance Tube. J. Aerospace Sci., Vol. 26, No. 10, 1959, pp. 684-685.

14. Shapiro, A. H. On the Maximum Attainable Temperature in Resonance Tubes. J. Aerospace Sci., Vol. 27, No. 1, 1960, pp. 66-67.

15. Vrebalovich, T. Resonance Tubes in a Supersonic Flow Field. Jet Propulsion Lab., Calif. Inst. of Tech. Report No. 32.378, 1962.

16. Sibulkin, M. Experimental Investigation of Energy Dissipation in a Resonance Tube. ZAMP, Vol. 14, 1963, pp. 495-703.

17. Reynolds, A. J. On Energy Separation by Aerodynamic Processes. J. Aerospace Sci., Vol. 28, 1961, pp. 244-245.

18. Brocher, E., C. Maresca and M. Albertini. Effect of Gas Properties on Thermal Effects in a Hartmann-Sprenger Tube. C. R. Acad. Sci., Vol. 273A, 1971, pp. 186-189.

19. Phillips, B. R. and A. J. Pavli. Resonance Tube Ignition of Hydrogen-Oxygen Mixtures. NASA TN D-6354, 1971.

20. Maresca, C. Study of Aerodynamic and Thermal Phenomena Occurring in Resonance Tubes. Thesis, Docteur-es-Sciences, University of Provence, Marseille, May 21, 1971.

21. Maresca, C. and E. Brocher. Mass Exchange in a Hartmann-Sprenger Tube. In preparation.

22. Brocher, E. and C. Maresca. Mechanism of Thermal Exchanges in a Resonance Tube. C. R. Acad. Sci., Vol. 271A, 1970, pp. 737-740.

23. Brocher, E. Hot Flow Length and Testing Time in Real Shock Tube Flow. Physics Fluids, Vol. 7, 1964, pp. 347-351.

24. Brocher, E. and C. Maresca. Approximate Calculation of Heat Transfer and Longitudinal Temperature Distribution at the Inlet of a Hartmann-Sprenger tube. C.R. Acad. Sci., Vol. 274A, 1972, pp. 1425-1428.

25. Eckert, E. R. G. Heat and Mass Transfer. McGraw-Hill, New York, 1959, pp. 209-213.

APPENDIX

(1) For a Mach number M_2 and a temperature ratio which are not too high, one can write with good approximation:

$$Re_2 \approx (\sqrt{\gamma}) M_2 Re^*.$$

The heat-transfer coefficient h_2 [Equation (12)] can then be put in the form:

$$h_2 = 0.023 \frac{\mu_2 C_p}{D} ((\sqrt{\gamma}) M_2 Re^*)^{0.8} Pr^{-0.6}. \tag{A.1}$$

Introducing Equations (A.1) and (11) into Equation (9), it becomes:

$$\frac{P_{cf}}{P_2} = \phi_{cf}[\gamma, M_2, L/D, Re^*] \left(\frac{\theta - 1}{\theta}\right) \tag{A.2}$$

where:

$$\phi_{cf} = 0{,}046 \left(\frac{\gamma}{\gamma - 1}\right) ((\sqrt{\gamma}) M_2 Re^*)^{-0.2} Pr^{-0.6} \left(\frac{L}{D}\right) \left(\frac{L_p}{L}\right) \times \left(\frac{1}{M_2} - \frac{a_2}{u_{ei}}\right) \left(1 + \frac{\gamma - 1}{2} M_2^2\right) I(K) \tag{A.3}$$

and

$$I(K) = \int_0^1 \left[\frac{(1 - \eta)\eta}{1 - \eta + K\eta^4}\right] d\eta. \tag{A.4}$$

The function I(K) is shown in Figure 21.

(2) The coefficient of friction C_{f2} [Equation (17)] can be written: /547

$$C_{f_2} = 0{,}316 ((\sqrt{\gamma}) M_2 Re^*)^{-0.25}.$$

Introducing Relations (16a) and (16b) into the integral appearing in Equation (15), one obtains:

$$\frac{P_{fr}}{P_2} = 0{,}079 \gamma ((\sqrt{\gamma}) M_2 Re^*)^{-0.25} \left(\frac{L}{D}\right) M_2^2 I(M_2) \tag{A.5}$$

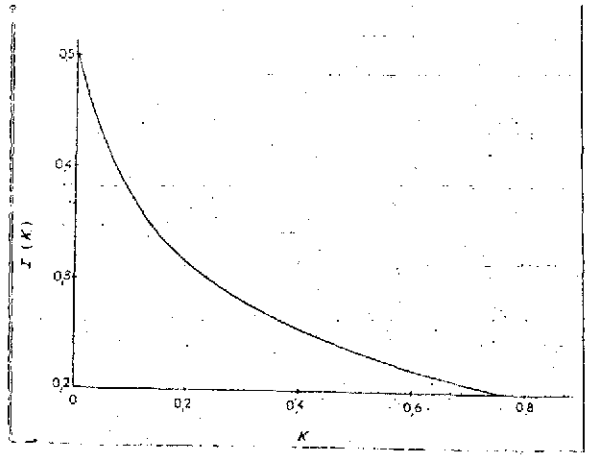

Figure 21. I(K) integral

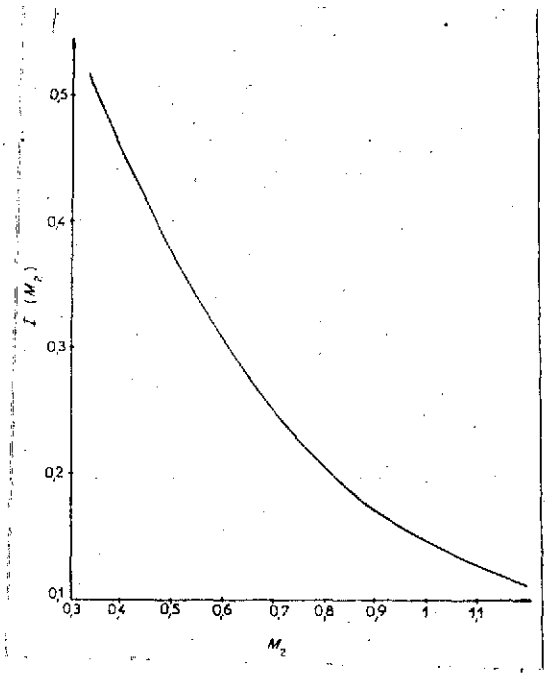

Figure 22. $I(M_2)$ function

where:

$$I(M_2) = \left(\frac{1}{M_2} - \frac{a_2}{u_{ci}}\right) \int_0^{L_p/L} \left(\frac{x}{L}\right) d\left(\frac{x}{L}\right) + \left(\frac{a_2}{u_{ci}} + \frac{a_2}{u_{cr}}\right) \times \int_{L_p/L}^{1} \left(1 - \frac{x}{L}\right) d\left(\frac{x}{L}\right)$$

$$= \frac{1}{2}\left[\left(\frac{1}{M_2} - \frac{a_2}{u_{ci}}\right)\left(\frac{L_p}{L}\right)^2 + \left(\frac{a_2}{u_{ci}} + \frac{a_2}{u_{cr}}\right) \times \left(1 - \frac{L_p}{L}\right)^2\right] \quad \text{(A.6)}$$

The function $I(M_2)$ is shown in Figure 22. The values of $I(M_2)$ are calculated for $\gamma = 7/5$ and $\gamma = 5/3$, but the difference between the two values is insignificant, and a single curve can be drawn.

The energy dissipated by friction can thus be written:

$$\frac{P_{fr}}{P_2} = \phi_{fr}[\gamma, M_2, L/D, Re^*] \quad \text{(A.7)}$$

where

$$\phi_{fr} = 0.079\gamma((\sqrt{\gamma})M_2 Re^*)^{-0.25}\left(\frac{L}{D}\right) M_2^2 I(M_2). \quad \text{(A.8)}$$